1
2
3
4
5
6
7
8
9
10
11
12
13
14
15
16
17
18
19
20
21
22
23
24
25
26
27
28
29
30
31
32
33
34
35
36
37
38
39
40
41
42
43
44
45
46
47
48
49
50
51
52
53
54
55
56
57
58
59
60

Spin-Hall magnetoresistance in multidomain helical spiral systems

A. Aqeel, M. Mostovoy, B. J. van Wees and T. T. M. Palstra

Zernike Institute for Advanced Materials, University of Groningen, Nijenborgh 4, 9747 AG Groningen, The Netherlands

E-mail: `a.aqeel@rug.nl`, `t.t.m.palstra@rug.nl`

October 2016

Abstract. We study the spin-Hall magnetoresistance (SMR) in a multidomain helical spiral magnet Cu_2OSeO_3|Pt heterostructures. We compare the SMR response of Cu_2OSeO_3 at 5 K, when the magnetic domains are almost frozen, to that at elevated temperatures, when domain walls move easily. At 5 K the SMR amplitude vanishes at low applied magnetic fields, while at 50 K it does not. This phenomenon can be explained by the effect of the magnetic field on the domain structure of Cu_2OSeO_3. At elevated temperatures the system can reach the thermodynamic equilibrium state, in which a single domain that has a minimal energy for a given field direction occupies the whole sample and gives rise to a nonzero SMR signal. In contrast at 5K, the three types of domains with mutually orthogonal spiral wave vectors have equal volumes independent of the field direction, which leads to the cancellation of the SMR signal at low fields. In the single-domain conical spiral and collinear ferrimagnetic states, the angular and field dependence of the SMR is found to be same at all temperatures ($T \leq 50$ K). This behavior can be understood within the framework of the SMR theory developed for collinear magnets.

1. Introduction

The recently discovered magnetoresistance phenomenon - known as the spin-Hall magnetoresistance (SMR) [1–3], has attracted considerable attention because of the possibility to electrically detect the magnetization of an insulating magnetic layer [4,5]. To measure the SMR, a simple device structure consisting of a heavy normal metal (NM) with a finite spin-Hall angle [6] on top of a ferromagnetic or ferrimagnetic (FM) insulator is used. The Hall resistance of the NM contact changes with the absorption/reflection of spin currents at the NM|FM interface [7,8]. The SMR has been mostly studied for collinear magnetic insulators including the prototype material – yttrium iron garnet (YIG) and, recently, more complex magnets, e.g. $CoFe_2O_4$ [5], $CoCr_2O_4$ [4] and $YGd_2Fe_4InO_{12}$ [9]. Among magnetic materials with complex magnetic orders, the noncollinear magnets with a broken space-inversion symmetry, known as chiral magnets, have the most fascinating physical properties. Chiral magnets show numerous phases

Spin-Hall magnetoresistance in multidomain helical spiral systems   2

with complex spin structures, such as the multidomain helical spiral state, the single-domain conical spiral state and the skyrmionic crystal state [10]. In these magnets, the relativistic Dzyaloshinskii-Moriya interaction between spins [11,12] results in a twist of the collinear ferromagnetic spin ordering, which stabilizes noncollinear chiral magnetic structures [13–16]. Examples of such magnets are: MnSi [10,17], $Mn_{1-x}Fe_xGe$ [18], FeGe [19–21], $Fe_{1x}Co_xSi$ [22] and Cu_2OSeO_3 [23–27]. Among these chiral magnets, Cu_2OSeO_3 is the first magnetic insulator ($T_c = 58$ K) in which magnetic skyrmions are experimentally observed [23–25]. To detect non-collinear chiral magnetic structures in these systems, sophisticated experimental techniques, such as Lorentz transmission electron microscopy, are used [23]. Recently, it has been shown that the SMR is an effective tool for all-electric detection of canted spin states in frustrated magnets [9] and complex spin structures in chiral magnetic insulators [28].

In this paper, we report a systematic study of the excitation and detection of spin currents in the multidomain helical spiral system Cu_2OSeO_3 using the SMR. Cu_2OSeO_3 is a cubic chiral magnet showing a variety of noncollinear magnetic phases [see Fig 1(a)]. At zero and low applied magnetic fields the magnetic state of Cu_2OSeO_3 is the helical spiral state with a period of 50 nm [23]. This is a multidomain magnetic state, as the spiral wave vector $\boldsymbol{Q}$ can be oriented along any of the three equivalent crystallographic directions: [100], [010] or [001]. When the external magnetic field exceeds the lower critical field ($H \geq H_{c1}$), the multidomain state transforms into a single-domain conical spiral state with the spiral wave vector $\boldsymbol{Q}$ oriented along the applied field $\boldsymbol{H}$. The cone angle θ of the spiral decreases with increasing magnetic field and becomes zero above the second-critical field ($H \geq H_{c2}$), which corresponds to the field-induced collinear ferrimagnetic (FM) state [see Fig. 1(a)]. We reported previously the field dependence of the SMR in different magnetic phases of Cu_2OSeO_3 at 5 K [28]. Here, we study the angular and field dependence of the SMR at elevated temperatures (25 K and 50 K) focusing on effects of the transformations from the multidomain helical spiral state into the single-domain conical spiral state and then to the collinear ferrimagnetic state. We find interesting differences between the SMR responses of Cu_2OSeO_3 at low and high temperatures.

2. Experimental procedure

Cu_2OSeO_3 single crystals of typical dimensions $\approx 4mm \times 4mm \times 2mm$ were grown by a chemical vapor transport method [29,30]. The structure was characterized by a Bruker D8 Venture single crystal x-ray diffractometer. The same diffractometer was used to orient the crystals along [111] direction, followed by the polishing step on (111) surfaces to obtain the surface roughness around 2 nm. The Hall-bar device structures were patterned on the polished (111) crystal surface of Cu_2OSeO_3 by using e-beam lithography. In these patterned Hall-bars 5 nm thick Platinum (Pt) was deposited by dc sputtering. To check the surface roughness and thickness of deposited metallic layers,
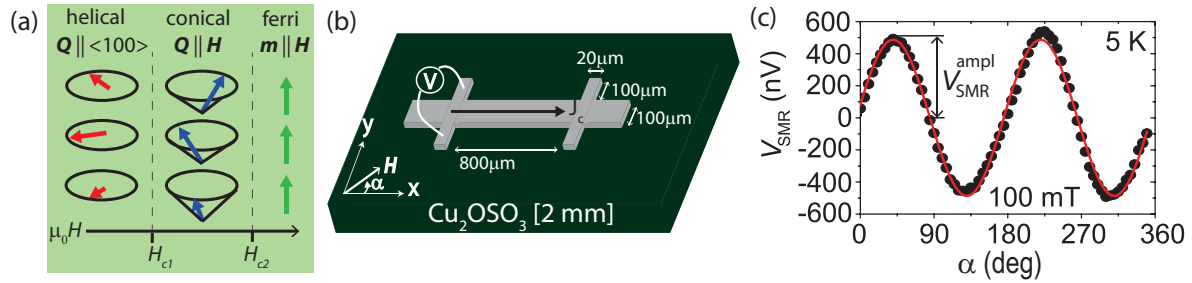
Spin-Hall magnetoresistance in multidomain helical spiral systems   3

Figure 1. (a) Schematic illustration of the types of field-induced magnetic order in the Cu_2OSeO_3 single crystal. Here $\boldsymbol{H}$, $\boldsymbol{Q}$ and $\boldsymbol{m}$ represent the applied magnetic field, the spiral wave vector and magnetization unit vector of Cu_2OSeO_3, respectively. H_{c1} and H_{c2} represent the fields at which the magnetic transitions occur in Cu_2OSeO_3. (b) Device configuration for the transverse resistance measurement of the Pt film on top of Cu_2OSeO_3. (c) Angular dependence of the SMR signal (V_{SMR}) at 5 K in ferrimagnetic state of Cu_2OSeO_3. Here, the solid line shows a $\sin(2\alpha)$ fit.

atomic force microscopy was used.

All electrical measurements were performed in the transverse Hall-bar configuration [see Fig. 1(b)], in a quantum design Physical Properties Measurement System (PPMS). A Stanford SR-830 lock-in amplifier is used to measure the first harmonic signal at a reference frequency of 17 Hz. The current (1 mA) was sent to the device using a custom-built current source and the response signal was pre-amplified, before sending it back to the lock-in amplifier. The angular dependence of the sample response was recorded by rotating it in the superconducting magnet of the PPMS with the magnetic field varying in the xy-plane of the device, as shown in Fig 1(b).

3. Results and discussion

When current I is sent through the Pt Hall-bar, a transverse spin current is generated due to the spin-Hall effect (SHE) [31–33], resulting in a spin accumulation, $\boldsymbol{\mu}_s$, at the Pt|Cu_2OSeO_3 interface. When $\boldsymbol{\mu}_s$ is perpendicular to the magnetization $\boldsymbol{M}$ of Cu_2OSeO_3, the spin current from the Pt contact to Cu_2OSeO_3 will be partially absorbed at the interface because of the spin torque effect, resulting in a higher resistance of the Pt contact. When $\boldsymbol{\mu}_s \parallel \boldsymbol{M}$, the spin torque effect vanishes and the spins are reflected back into the Pt contact. The reflected spins generate an additional charge current through the inverse spin-Hall effect (ISHE), resulting a smaller resistance. When $\boldsymbol{M}$ makes an angle with $\boldsymbol{\mu}_s$, the additionally generated charge current due to the ISHE results in both longitudinal and transverse responses. The latter gives rise to the SMR signal presented here.

Spin-Hall magnetoresistance in multidomain helical spiral systems 4

When the applied magnetic field $\boldsymbol{H}$ is rotated in the Pt film plane and the magnetization $\boldsymbol{M}$ fully aligns along $\boldsymbol{H}$, a periodic angular dependence $\sin(2\alpha)$ of the transverse Pt resistance is observed, where α is the angle between the applied current and $\boldsymbol{H}$, as shown in Fig. 1(b). The SMR is measured by detecting the angular dependence of the first-order response of the system, for which it is necessary to measure the first and third harmonics by the lock-in amplifier in the transverse configuration generated by the current I [4, 34]. As the third harmonic response is negligible, only the first harmonic signal of the lock-in amplifier is presented as the SMR signal V_{SMR}.
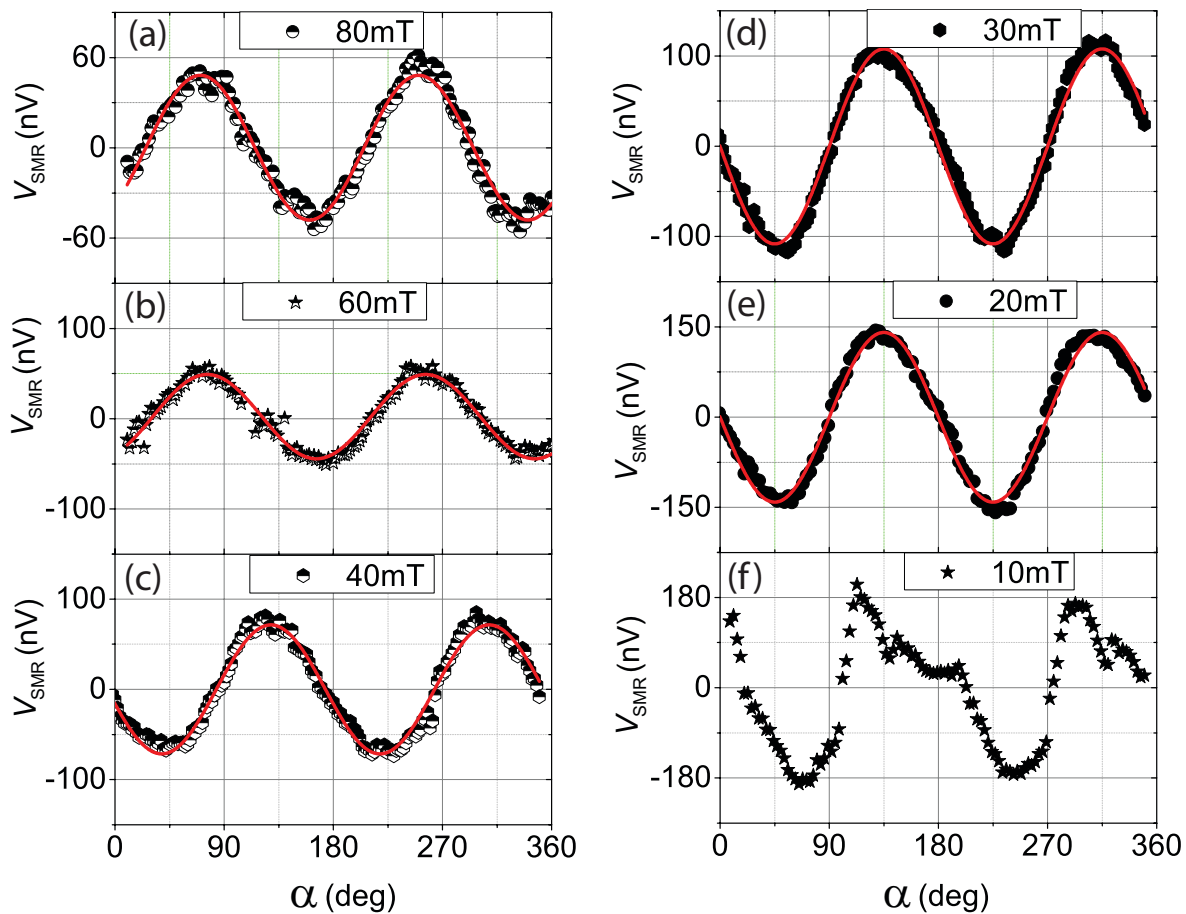

Figure 2. (a-f) Angular dependence of the SMR signal (V_{SMR}) at 50 K at different applied magnetic field strengths. The solid lines represent $\sin(2\alpha)$ fits.

Fig. 1(c) shows the SMR signal at 5 K in a magnetic field of 100 mT after subtraction of additional signal due to the ordinary Hall effect resulting from a slight misalignment of the sample. Fig. 1(c) shows a clear $\sin(2\alpha)$ angular dependence, as expected for the SMR. The angular dependence of the SMR in the ferrimagnetic state at temperatures higher than 5 K is also given by $\sin(2\alpha)$, as shown in Fig. 2(a). As the magnetic field decreases and the system undergoes a transition into the conical spiral state, the angular dependence of the SMR is still $\sin(2\alpha)$ [see Figs. 2(b) - 2(d)]. The notable feature observed in the conical spiral state is the sign change of the amplitude of the SMR signal,

Spin-Hall magnetoresistance in multidomain helical spiral systems   5

$V_{\mathrm{SMR}}^{\mathrm{ampl}}$ [cf. Figs. 2(a) and 2(b) with Figs. 2(c) and 2(d)]: $V_{\mathrm{SMR}}^{\mathrm{ampl}}$ decreases with decreasing field from a positive value at H_{c2} to a negative value at H_{c1}. In the helical spiral state, the sign of the SMR amplitude remains negative upon further decrease of the applied magnetic field, as shown in Figs. 2(e) and 2(f)]. In contrast, the angular dependence of the SMR in the helical state strongly deviates from the $\sin(2\alpha)$ [see Fig. 2(f)], consistent with the observations reported in literature [28]. A similar behavior is observed at 25 K in the conical phase: $V_{\mathrm{SMR}}^{\mathrm{ampl}}$ decreases with decreasing field from a positive value at H_{c2} to a negative value at H_{c1} [cf. Fig. 3(a) with Figs. 3(b) and 3(c)]. The angular dependence of the SMR deviates from $\sin(2\alpha)$ dependence at the conical spiral to helical spiral transition [see Fig. 3(d)]. In the helical state, sharp discontinuities and deviations from the $\sin(2\alpha)$ dependence are observed [see Figs. 3(e)-3(i)]. The SMR signal vanishes at zero field, as shown in Fig. 3(j).

The sign reversal of the SMR signal in the conical phase at 25 K and 50 K (shown in Figs. 2(c), 3(b) and 3(c) can be explained by using equation 1 from Ref. [28]:

$$V_{\mathrm{SMR}} \propto \langle m_x m_y \rangle = \frac{1}{4} \sin 2\alpha \left(3 \left(\frac{H}{H_{\mathrm{c2}}} \right)^2 - 1 \right) \tag{1}$$

where m_x and m_y represents the parallel and orthogonal in-plane components of the magnetization unit vector $\boldsymbol{m}$ with respect to the applied current direction, respectively. V_{SMR}^{ampl} remains constant for $H > H_{\mathrm{c2}}$ and decreases for $H < H_{\mathrm{c2}}$ by changing sign at $H = \frac{H_{\mathrm{c2}}}{\sqrt{3}}$ in good qualitative agreement with the experimental observations at different temperatures [see Figs. 4(a), 4(b) and 4(c)].

The spin configuration in the helical spiral state is complicated by the presence of three types of magnetic domains with different orientations of the spiral wave vector $\boldsymbol{Q}$. Moreover, in each domain the helix deforms under the applied magnetic field. Therefore, one can imagine three possible situations for a given H:

(i) three domains with three different orientations of $\boldsymbol{Q}$ occupy the same volume and equally contribute to the SMR;

(ii) The domains with different orientations of $\boldsymbol{Q}$ occupy different volumes and contribute to the SMR unequally;

(iii) The SMR signal comes from a single magnetic domain that has the lowest energy and occupies the whole sample.

In first scenario when all three domain occupy same volume and contribute equally to the SMR, the SMR signal vanishes in zero field due to cancellation of the contributions from the three types domains with mutually orthogonal spiral wave vectors $\boldsymbol{Q}$. Such a cancellation of the SMR signal in the multidomain state is observed at 5 K (see Fig. 4(c)). It is plausible that at low temperatures the domains are frozen and that the domain boundaries do not propagate in the rotating magnetic field, resulting in equal volumes of all three types of domains, which leads to cancellation of the SMR signal. When the magnetic field is increased above 20 mT at 5 K, the domain boundaries start to move and the helical spirals in each domain become distorted, resulting in a linear
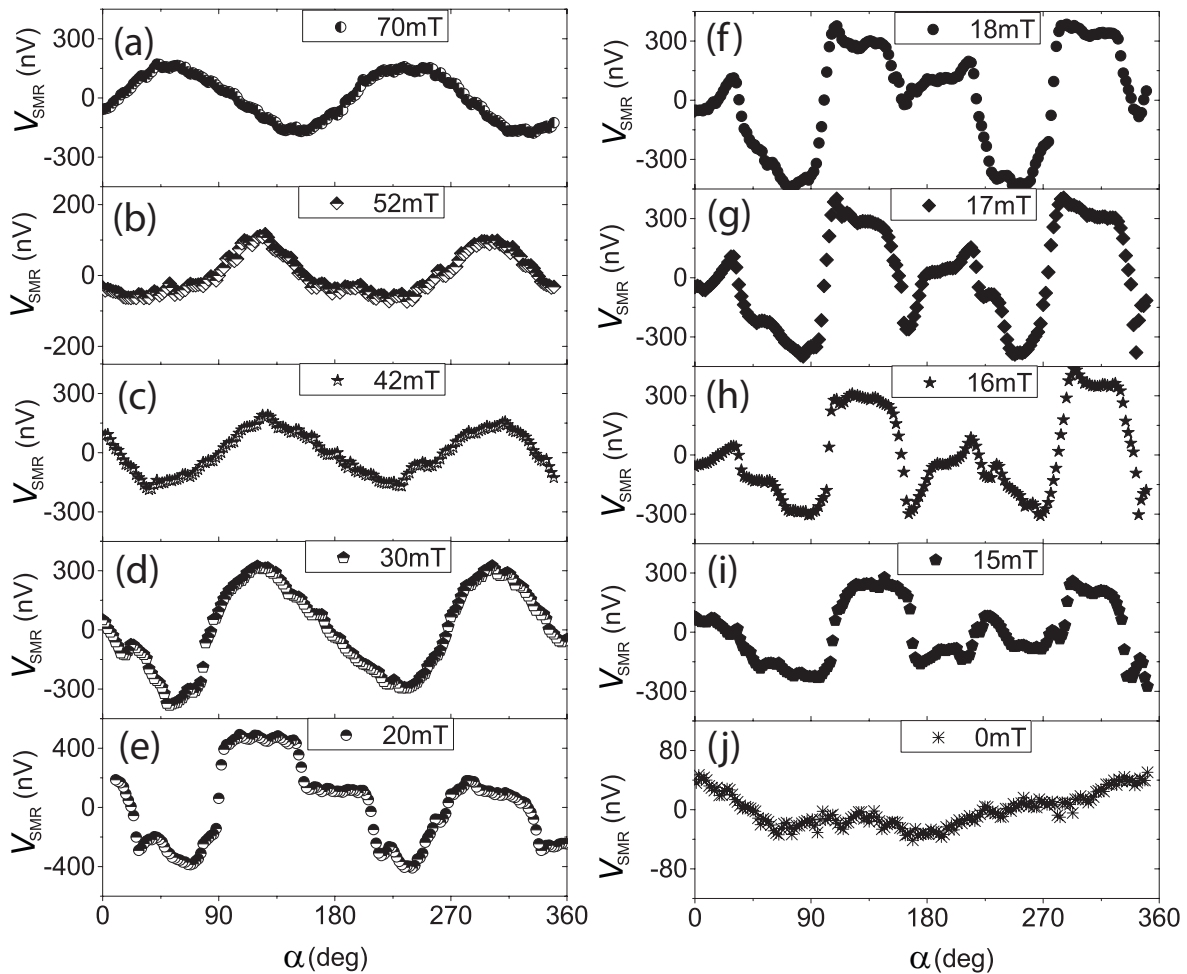
Spin-Hall magnetoresistance in multidomain helical spiral systems   6

Figure 3. (a-j) Angular dependence of the SMR signal (V_{SMR}) at 25 K at different applied magnetic field strengths.

increase of the SMR signal until H_{c1}, at which the material undergoes a transition into the conical spiral state [see Fig. 4(c)]. At 25 K the SMR also vanishes in low applied magnetic fields. Nevertheless, it vanishes at much lower fields ($H < 15$ mT) than at 5 K [cf. Figs. 4(b) and 4(c)]. The sample at 25 K may follow the second scenario in which the three types of domains occupy different volumes, which leads to a non-zero SMR signal. Only close to zero field the contributions from the three types of domains become equal and the cancellation occurs [see Fig. 4(b)].

At 50 K the SMR signal stays almost constant in the helical phase and does not vanish. The situation corresponds to third scenario, in which the magnetic domain with the lowest energy occupies the whole sample, resulting in a finite SMR signal V_{SMR} in the helical phase. This can be explained by the fact that at higher temperatures (50 K), thermal fluctuations facilitate the propagation of domain boundaries. If the domain boundaries move fast on the time scale of measurements of the angular dependence of the SMR signal ($\sim 2°/$min), the sample will always be in thermal equilibrium. In thermal equilibrium, the domain with the minimal energy occupies the whole sample, resulting
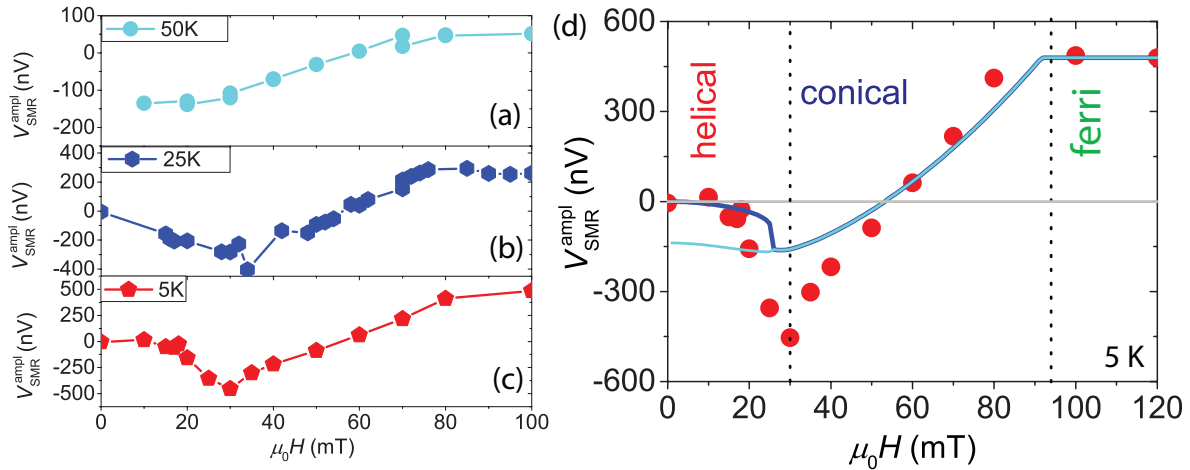
Spin-Hall magnetoresistance in multidomain helical spiral systems   7

Figure 4. Magnetic field dependence of the SMR signal (V_{SMR}) at (a) 50 K, (b) 25 K and (c) 5 K. (d) Field dependence of the V_{SMR} at 5 K with the transition between different magnetic states of the Cu_2OSeO_3 marked by vertical lines. The dark blue curve indicate the calculated amplitude of the SMR signal by considering equal contribution from three magnetic domains and the light blue curve is calculated by assuming that the system is in thermal equilibrium.

in a nearly constant SMR signal in the helical phase, as observed in Fig. 4(a). Fig. 4(d) shows the calculated fits at 5 K by considering the first scenario of frozen domains with equal contribution to the SMR signal and the third scenario with thermal equilibrium by using equation 1. Both calculated fits are same at higher applied magnetic fields, in the conical and field induced collinear ferrimagnetic states of Cu_2OSeO_3. The prominent differences appear in the multidomain helical state where the calculated amplitude of the SMR does not goes to zero by considering the system in the thermal equilibrium, consistent with the observation at 50 K [cf. Figs. 4(a) with 4(d)].

In conclusion, we demonstrated that the SMR can be used to electrically detect the inhomogeneous spin structures in the multidomain helical magnet Cu_2OSeO_3. We showed that the SMR can be used to describe the changes in the domain structure of Cu_2OSeO_3 in the helical spiral state at different temperatures. These findings constitute an important step forward in the emerging field of insulator spintronics, which holds promise of energy-efficient magnetic memory devices. Our approach can be used to detect and manipulate nanomagnetic structures, such as domain walls and skyrmions.

3.1. Acknowledgments

Spin-Hall magnetoresistance in multidomain helical spiral systems   8

References

[1] Vlietstra N, Shan J, Castel V, van Wees B J and Ben Youssef J 2013 *Phys. Rev. B* **87**(18) 184421

[2] Vlietstra N, Shan J, Castel V, Ben Youssef J, Bauer G E W and van Wees B J 2013 *Appl. Phys. Lett.* **103** 032401

[3] Nakayama H, Althammer M, Chen Y T, Uchida K, Kajiwara Y, Kikuchi D, Ohtani T, Geprägs S, Opel M, Takahashi S, Gross R, Bauer G E W, Goennenwein S T B and Saitoh E 2013 *Phys. Rev. Lett.* **110**(20) 206601

[4] Aqeel A, Vlietstra N, Heuver J A, Bauer G E W, Noheda B, van Wees B J and Palstra T T M 2015 *Phys. Rev. B* **92**(22) 224410

[5] Isasa M, Bedoya-Pinto A, Vélez S, Golmar F, Sánchez F, Hueso L E, Fontcuberta J and Casanova F 2014 *Appl. Phys. Lett.* **105** 142402

[6] Sagasta E, Omori Y, Isasa M, Gradhand M, Hueso L E, Niimi Y, Otani Y and Casanova F 2016 *Physical Review B* **94**(6) 060412

[7] Chen Y T, Takahashi S, Nakayama H, Althammer M, Goennenwein S T B, Saitoh E and Bauer G E W 2013 *Phys. Rev. B* **87**(14) 144411

[8] Jia X, Liu K, Xia K and Bauer G E W 2011 *Europhys. Lett.* **96** 17005 ISSN 0295-5075, 1286-4854

[9] Ganzhorn K, Barker J, Schlitz R, Piot B A, Ollefs K, Guillou F, Wilhelm F, Rogalev A, Opel M, Althammer M, Geprägs S, Huebl H, Gross R, Bauer G E W and Goennenwein S T B 2016 *Phys. Rev. B* **94**(9) 094401

[10] Mühlbauer S, Binz B, Jonietz F, Pfleiderer C, Rosch A, Neubauer A, Georgii R and Böni P 2009 *Science* **323** 915–919

[11] Dzyaloshinsky I 1958 *J. Phys. Chem. Solids* **4** 241 – 255 ISSN 0022-3697

[12] Moriya T 1960 *Phys. Rev.* **120**(1) 91–98

[13] Nagaosa N and Tokura Y 2013 *Nature Nanotech.* **8**(12) 899–911 ISSN 1748-3387

[14] Braun H B 2012 *Adv. Phys.* **61** 1–116

[15] Tokura Y and Seki S 2010 *Adv. Mater.* **22** 1554–1565 ISSN 1521-4095

[16] Kimura T 2012 *Annu. Rev. Condens. Matter Phys.* **3** 93–110

[17] Jonietz F, Mühlbauer S, Pfleiderer C, Neubauer A, Münzer W, Bauer A, Adams T, Georgii R, Bni P, Duine R A, Everschor K, Garst M and Rosch A 2010 *Science* **330** 1648–1651

[18] Shibata K, Yu X Z, Hara T, Morikawa D, Kanazawa N, Kimoto K, Ishiwata S, Matsui Y and Tokura Y 2013-10 *Nature Nanotech.* **8** 723–8

[19] Yu X Z, Kanazawa N, Onose Y, Kimoto K, Zhang W Z, Ishiwata S, Matsui Y and Tokura Y 2011 *Nature Mater.* **10** 106–109

[20] Wilhelm H, Baenitz M, Schmidt M, Rößler U K, Leonov A A and Bogdanov A N 2011 *Phys. Rev. Lett.* **107**(12) 127203

[21] Moskvin E, Grigoriev S, Dyadkin V, Eckerlebe H, Baenitz M, Schmidt M and Wilhelm H 2013 *Phys. Rev. Lett.* **110**(7) 077207

[22] Münzer W, Neubauer A, Adams T, Mühlbauer S, Franz C, Jonietz F, Georgii R, Böni P, Pedersen B, Schmidt M, Rosch A and Pfleiderer C 2010 *Phys. Rev. B* **81**(4) 041203

[23] Seki S, Yu X Z, Ishiwata S and Tokura Y 2012 *Science* **336** 198–201

[24] Seki S, Kim J H, Inosov D S, Georgii R, Keimer B, Ishiwata S and Tokura Y 2012 *Phys. Rev. B* **85**(22) 220406

[25] Adams T, Chacon A, Wagner M, Bauer A, Brandl G, Pedersen B, Berger H, Lemmens P and Pfleiderer C 2012 *Phys. Rev. Lett.* **108**(23) 237204

[26] Versteeg R B, Vergara I, Schäfer S D, Bischoff D, Aqeel A, Palstra T T M, Grüninger M and van Loosdrecht P H M 2016 *Phys. Rev. B* **94**(9) 094409

[27] Qian F, Wilhelm H, Aqeel A, Palstra T T M, Lefering A J E, Brück E H and Pappas C 2016 *Phys. Rev. B* **94**(6) 064418

[28] Aqeel A, Vlietstra N, Roy A, Mostovoy M, van Wees B J and Palstra T T M 2016 *Phys. Rev. B* **94**(13) 134418

1
2
3
4
5
6
7
8
9
10
11
12
13
14
15
16
17
18
19
20
21
22
23
24
25
26
27
28
29
30
31
32
33
34
35
36
37
38
39
40
41
42
43
44
45
46
47
48
49
50
51
52
53
54
55
56
57
58
59
60

Spin-Hall magnetoresistance in multidomain helical spiral systems   9

[29] Belesi M, Rousochatzakis I, Wu H C, Berger H, Shvets I V, Mila F and Ansermet J P 2010 *Phys. Rev. B* **82**(9) 094422

[30] Aqeel A, Baas J, Blake G R and Palstra T T M 2016 *unpublished*

[31] Kato Y K, Myers R C, Gossard A C and Awschalom D D 2004 *Science* **306** 1910–1913 ISSN 0036-8075

[32] Wunderlich J, Kaestner B, Sinova J and Jungwirth T 2005 *Phys. Rev. Lett.* **94**(4) 047204

[33] Sinova J, Valenzuela S O, Wunderlich J, Back C H and Jungwirth T 2015 *Rev. Mod. Phys.* **87**(4) 1213–1260

[34] Vlietstra N, Shan J, van Wees B J, Isasa M, Casanova F and Ben Youssef J 2014 *Phys. Rev. B* **90**(17) 174436